Average hydrodynamic correction for the Brownian dynamics calculation of flocculation rates in concentrated dispersions

German Urbina-Villalba,* Máximo García-Sucre, and Jhoan Toro-Mendoza
Centro de Física, Laboratorio de Fisicoquímica de Coloides, Instituto Venezolano de Investigaciones Científicas (IVIC), Apartado 21827, Caracas, Venezuela

(Received 3 June 2003; published 31 December 2003)

In order to account for the hydrodynamic interaction (HI) between suspended particles in an average way, Honig *et al.* [J. Colloid Interface Sci. **36**, 97 (1971)] and more recently Heyes [Mol. Phys. **87**, 287 (1996)] proposed different analytical forms for the diffusion constant. While the formalism of Honig *et al.* strictly applies to a binary collision, the one from Heyes accounts for the dependence of the diffusion constant on the local concentration of particles. However, the analytical expression of the latter approach is more complex and depends on the particular characteristics of each system. Here we report a combined methodology, which incorporates the formula of Honig *et al.* at very short distances and a simple local volume-fraction correction at longer separations. As will be shown, the flocculation behavior calculated from Brownian dynamics simulations employing the present technique, is found to be similar to that of Batchelor's tensor [J. Fluid. Mech. **74**, 1 (1976); **119**, 379 (1982)]. However, it corrects the anomalous coalescence found in concentrated systems as a result of the overestimation of many-body HI.

DOI: 10.1103/PhysRevE.68.061408 PACS number(s): 82.70.Kj, 82.70.Dd, 02.70.Ns, 05.40.Jc

INTRODUCTION

Brownian Dynamics (BD) has been used for more than 20 years to describe the behavior of suspensions [1–7]. Its applications span a wide variety of problems ranging from protein adsorption [8,9], sedimentation [10], heteroaggregation [11], and more recently flocculation rates in both suspensions [12–14] and emulsions [15–19]. Probably the most severe limitations of BD are [20–22] (a) the small time step required to account for the typical short-range potentials of the interacting particles and (b) the large computational power required for the proper account of hydrodynamic interactions (HI's). Despite these shortcomings and the fact that new computational techniques permit the calculation of a larger number of mesoscopic particles [23,24], BD is still widely used. This is partially due to the close resemblance between the movement of particles in real systems and in their simulated analogs. Such parallelism allows direct comparison of the results with well-known analytical equations from statistical treatments [25–28]. More importantly, these similarities allow easy incorporation of physicochemical effects at a lower length scale. BD is particularly useful for the simulation of emulsions where surfactant adsorption, interfacial movement, surface deformation, film drainage, and even fluid-mediated mass transfer between separated drops can occur [29,30].

THEORETICAL EXPRESSIONS FOR HYDRODYNAMIC INTERACTIONS IN CONCENTRATED DISPERSIONS

Hydrodynamic effects can cause like-charge attraction between suspended particles near a wall [31,32], originate pathological behaviors in sheared systems of hard spheres [33], favor the formation of open structures during aggregation [34], and even enhance the diffusivity of colloids [35,36]. In the *diffusion* formulation, where the velocity of a particle, $\mathbf{V}$, is calculated from the total force acting over each particle, $\mathbf{V}=\mathbf{D}\cdot\mathbf{F}$ [20], the general form of the diffusion matrix is [37,38]

$$D_{ii}=D_0\hat{I}+D_0\sum_{j=1,j\neq i}\{A_s(r_{ij})\hat{r}_{ij}\hat{r}_{ij}+B_s(r_{ij})[\hat{I}-\hat{r}_{ij}\hat{r}_{ij}]\}, \tag{1}$$

$$D_{ij}=D_0\{A_c(r_{ij})\hat{r}_{ij}\hat{r}_{ij}+B_c(r_{ij})[\hat{I}-\hat{r}_{ij}\hat{r}_{ij}]\}, \tag{2}$$

where D_0 is the diffusion (Stokes) coefficient of a solid particle at infinite dilution

$$D_0=\frac{kT}{6\pi\eta a_i}, \tag{3}$$

η is the solvent viscosity, T the temperature, k the Boltzmann constant, and a_i the radius of particle i. The scalar functions A_s, B_s, A_c, and B_c in Eqs. (1) and (2) are referred to as (self: $i=j$, and cross: $i\neq j$) mobility functions, $\hat{\mathbf{r}}_{ij}=\mathbf{r}_{ij}/r_{ij}$ and $\mathbf{r}_{ij}=\mathbf{r}_i-\mathbf{r}_j$. Taylor expansion of the diffusion matrix is equivalent to Taylor expansion of its mobility functions. These are calculated supposing pairwise additive interactions, and their most usual forms are Oseen [37], Rotne-Prager [39], and Batchelor [40,41] expressions, the latter usually referred as the *exact* mathematical form.

In the BD algorithm from Ermak and McCammon [1], the elements of the diffusion matrix are explicitly included into the equation of motion. Following the original notation [1]

$$r_k=r_k^0+\sum_l\frac{\partial D_{kl}^0}{\partial r_l}\Delta t+\sum_l\frac{D_{kl}^0F_l^0}{kT}\Delta t+R_k(\Delta t), \tag{4}$$

*Author to whom correspondence should be addressed. Electronic address: guv@ivic.ve

where r_k is the position of particle k, superscript "0" indicates the value of that variable at the beginning of the time step (Δt), $R_k(\Delta t)$ is a random displacement with a Gaussian distribution, and variance $2D_{kl}\Delta t$, and subscripts k and l span all directions (x,y,z) and particles. F_l is the sum of interparticle and external forces acting in direction l.

From the computational point of view, Eq. (4) presents two fundamental difficulties: (a) the gradient of the diffusion matrix, and (b) given the form of the tensor [Eqs. (1) and (2)], the HI couples the random deviates of each particle $R_k(\Delta t)$ to all other particles in the system. Whenever mobility functions depend on the relative distance between the particles and not on their positions, the second term on the right-hand side of Eq. (4) is equal to zero. Several strategies had been suggested for the generation of random deviates, including Cholesky decomposition, QR decomposition, Chebyshev polynomial approximation, etc. [1,42–44]. As originally pointed out by Ermak and McCammon [1] those methodologies depend on the configuration and the polydispersity [37] of the particles. Cholesky methodology, in particular, fails invariably in emulsion stability simulations (ESS's) with volume fractions above 1% ($\phi > 0.01$). Thus, it is commonly used for calculations with a limited number of particles and low ϕ.

Starting from exact expressions deduced by Brenner [45,46] for the HI between a sphere and either a plane surface [45] or another sphere of equal radius (a) [45,46], Honig *et al.* [47] proposed an average correction for the diffusion constant $D(u)$ of a particle during a binary encounter:

$$D(u) = \frac{D_0}{\beta(u)}. \tag{5}$$

Equation (5) is based on an approximate rational function which has the correct values and limiting slopes for large and small distances $d(d/a = u)$ between the particles:

$$\beta(u) = \frac{6u^2 + 13u + 2}{6u^2 + 4u}. \tag{6}$$

The function β takes the values of 1.08, 2.03, 7.83, at $u = 18.14$, 1.09, 0.091, respectively, going as high as 202.5 at $u = 0.0025$. It has been reported that similar rational functions [48] can reproduce the exact mobility functions with an accuracy of four figures for $u \geqslant 0.1$ and three figures for $0.01 \leqslant u < 0.1$ [45,46,48].

Old as well as up-to-date findings had been interpreted in terms of tensors (Oseen [49,50], Rotne-Prager [36,51], and Batchelor [32,52,53], as well as average functions (Honig [54,55]). However, these approximations overestimate the effect of HI's in concentrated systems where screening occurs [37]. This was pointed out by Bacon *et al.* [2,56] who used Batchelor tensor to demonstrate that pairwise additivity can even generate negative diffusion constants above a critical volume fraction (equal to 0.45 for hard spheres) [56]. Similarly, it can predict negative sedimentation speeds for $\phi = 0.27$ [2,56,57]. Such screening of long-range HI's was recently observed in suspensions of charged silica particles [58].

While average expressions [Eq. (6)] are able to describe HI's between two particles with great accuracy, they are unable to account for many-body interactions with appropriate consideration of the screening phenomena. Fortunately, the dependence of self-diffusion coefficients (in the short-time limit D_S^S) with respect to the volume fraction can be deduced from light scattering measurements [59–62]. Those results had been compared with theoretical expressions deduced from the average of mobility functions over two- and three-particle distribution functions [63–66]. It was found that the experimental data follows the prediction of Eq. (7) with different degrees of accuracy, depending on the volume fraction of internal phase [65,66]:

$$D(\phi) = D_0(1 - 1.73\phi - 0.93\phi^2 + 1.80\phi^2 + \cdots). \tag{7}$$

The ϕ^2 term in Eq. (7) contains two distinct contributions due to two-body hydrodynamic interactions ($-0.93\phi^2$) and three-body contributions ($+1.80\phi^2$). For $\phi < 0.30$, the second-order (two-body) expansion of the diffusion constant appears to be more reliable. At higher volume fractions, the trend is adequate but sizable differences are observed [60].

In order to account locally for many-body hydrodynamics, Heyes [20] recently proposed a configuration-dependent friction coefficient $\xi_i(\mathbf{R}) = kT/D$:

$$\xi(\mathbf{R}) = \xi_0 \left\{ 1 + C\left[\sum_{i \neq j} \varepsilon \left(\frac{\sigma}{r_{ij}} \right)^m \right] \right\}, \tag{8}$$

where ξ_0 is the friction coefficient at infinite dilution, $C = C(\phi)$ is a constant which depends on the volume fraction and is fitted with experimental data, m is an arbitrary exponent, σ is the hard-sphere diameter of the particles, and ε ($\sim$kT) sets the energy scale. As pointed out by Heyes [20], the interactions considered are pairwise additive, and they are not expected to go beyond the first coordination shell.

Equation (8) is well suited for Brownian dynamics simulations since it does not requires matrix inversions or correlated Brownian forces. In this approximation, Eq. (4) simplifies considerably. The final expression is equal to the Brownian dynamics equation in the absence of HI's:

$$r(t + \Delta t) = r(t) + \frac{F(t)\Delta t}{\xi(\mathbf{R})} + R(\xi(\mathbf{R})), \tag{9}$$

where $R(\xi(\mathbf{R}))$ is again a random variable with a Gaussian distribution.

The purpose of this communication is to provide a much simpler HI correction for BD simulations, which incorporates the exactness of Eqs. (5) and (6) for binary collisions, with the average volume fraction behavior predicted by Eq. (7).

MODEL

Figure 1 shows a schematic representation of the proposed model. In order to calculate HI's, an internal (R_{int}) and an external (R_{ext}) radii are ascribed to each particle. These radii divide the space in three sections. The HI's coming from particles in the outermost region $d > R_{\text{ext}}$ (where d is the

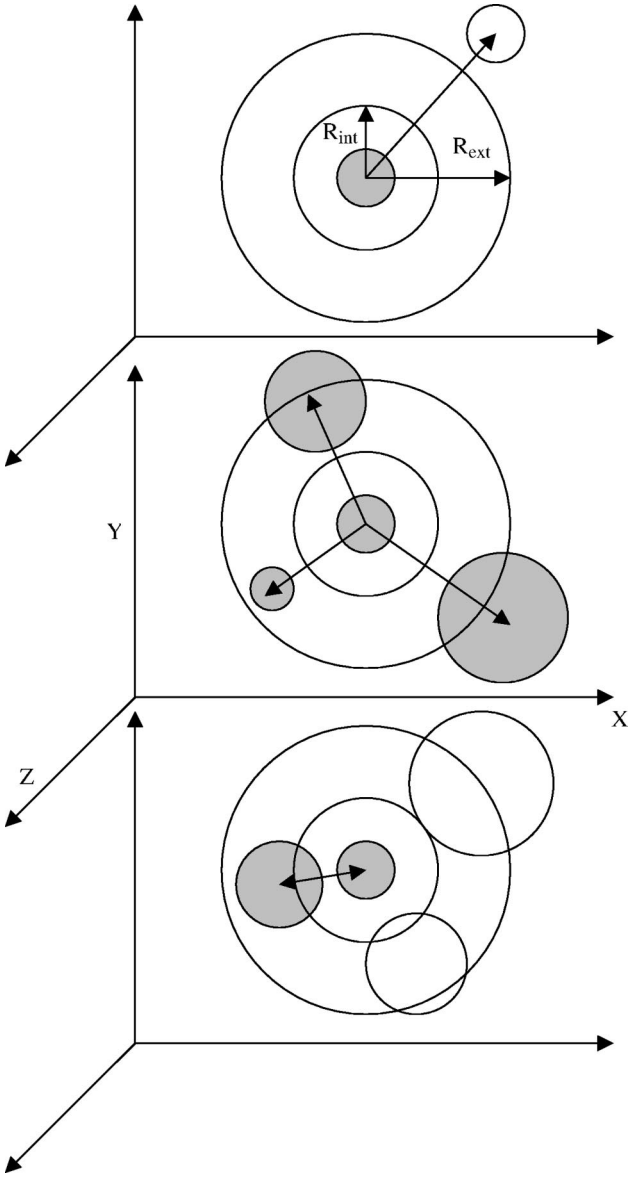

FIG. 1. Local evaluation of the volume fraction around a central particle (*C*). For clarity, only a transverse (*XY*) cut of the three-dimensional situation is shown. In order to calculate the effect of hydrodynamic interactions (HI's) on the movement of *C*, two distances (internal and external) are defined. Particles beyond R_{ext} do not influence the movement of *C* (upper picture). Particles between R_{int} and R_{ext} contribute with a fraction of their volume to the calculation of a local volume fraction ϕ around particle *C* (middle picture). Equation (7) can then used to calculate an effective diffusion constant $D(\phi,d)$ for *C*. However, since close-range HI's are much more significant than long-range ones, the approach of Honig *et al.* [47] is used instead whenever there is at least one neighbor particle (or a fraction of it) within the inner region $d \leqslant R_{int}$ (lower picture). If several particles are located within R_{int} at a given time, only the closest one is taken into account to calculate β and $D(\phi,d)$ [Eqs. (5) and (6)].

distance between the surface of the central particle and the surface of its neighbor, $d=r_{ij}-a_i-a_j$) are disregarded. They do not contribute to the hydrodynamic corrections of the central particle either because they are too far away to

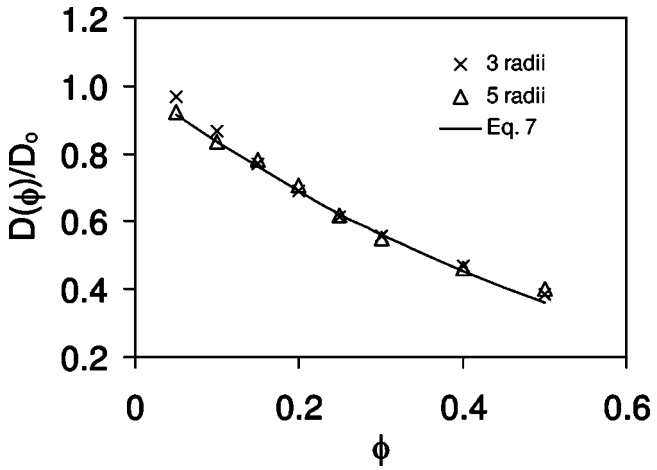

FIG. 2. In order to validate the geometrical procedure defined in Fig. 1, cubic cells of $0.05 \leqslant \phi \leqslant 0.50$ were built. External radii of $5a$ and $3a$ ($a=3.9\ \mu$m) were defined around a central particle *C*. In either case, the local volume fraction estimated by the geometrical procedure (Fig. 1) came out to be very close to the volume fraction of particles within the entire cell. Hence, the values of $D(\phi,d)$ calculated are very similar.

interact significantly or due to the screening of their HI's by closer particles.

Particles in the intermediate and inner regions contribute to the HI's of the central particle in different ways. Whenever a whole particle or a fraction of its volume penetrates the intermediate region (middle picture in Fig. 1), its volume inside this region ($R_{int} < d \leqslant R_{ext}$) is geometrically calculated. Once the total volume of particles within the intermediate region is calculated, the total volume fraction (ϕ) of particles within $0 \leqslant d \leqslant R_{ext}$ is computed (including the volume of the central particle). The diffusion constant of the central particle can then be calculated from Eq. (7), using terms accounting for two-body HI's up to second order in the volume fraction expansion [60–62,65,66].

In order to validate the geometrical procedure previously described for the local evaluation of ϕ [and $D(\phi)$], cubic cells of 125 particles orderly arranged were built. The volume fraction of particles in each cell (ϕ_{cell}) can be trivially calculated and $D(\phi)$ estimated according to Eq. (7). Alternatively, an external radius (R_{ext}) can be defined around a central particle in the cell and $D(\phi)$ estimated as a function of its *local* ϕ. The local volume fraction [and consequently $D(\phi)$] comes out to be similar to ϕ_{cell} (Fig. 2). Similar results are obtained for $R_{ext}=3a$ or $5a$. Notice that at $\phi=0.50$, $D(\phi)$ decreases from D_0 to $0.20D_0$. On the other hand, the correction of Honig *et al.* can reduce $D(u)$ from D_0 to $0.005D_0$ during a binary collision. Hence, if there is at least one particle within the inner region of a given central particle ($d \leqslant R_{int}$), the expression of Honig *et al.* [Eqs. (5) and (6)] is used to calculate the diffusion constant of the central particle regardless of the volume fraction of particles in the intermediate and outermost regions. If there are more than one particle within the inner region, only the closest one is used to compute β from Eq. (6).

In summary, the local volume fraction around each par-

ticle is used to compute its average diffusion constant. However, as can be inferred from the values of Eq. (6) at close distances and those of Eq. (7) at very high ϕ, the binary interaction is much more significant at short range. Thus, it is solely considered whenever it is present.

COMPUTATIONAL DETAILS

Using the above-mentioned approximations, the BD expression for the equation of motion of particle *i* subject to the average HI is

$$r_i(t+\Delta t)=r_i(t)+\frac{D_i(\phi,d)F_i\Delta t}{kT}+R(D_i(\phi,d)), \quad (10)$$

where $R(D_i(\phi,d))$ is a Gaussian function with zero mean and variance $6D_i(\phi,d)\Delta t$. As in the case of Heyes [20], this is equivalent to the BD algorithm in the absence of HI's, except for the presence of an effective diffusion coefficient.

Notice that in Eq. (10) the random deviates of each particle are now decoupled from one another [see Eq. (4)]. This simplifies the BD algorithm considerably. In dissipative particle dynamics (DPD) [23,24], the random force is only uncorrelated between different pairs of mesoscopic particles. In that case, ''fluid'' particles interact with dissipative, random, and conservative forces. These forces are connected through versatile relations which allow the system to reach equilibrium and even satisfy detailed balance in the limit of infinitesimal time steps ($\Delta t\rightarrow 0$) [67]. In a BD simulation, the magnitude of the thermal exchange between the particles and the solvent is determined by the size of the random contributions. These random deviates depend on the time step and are coupled to the conservative forces through the diffusion matrix [third term on the right-hand side of Eq. (4)]. In Ref. [15] we studied the variation of the thermal exchange between the particles and the fluid in the absence of HI's. It was found that in order to reproduce the value of the diffusion constant at infinite dilution [Eq. (3)] employing a well-behaved Gaussian routine, considerably large values of the thermal exchange are required. Since HI's slow down particle motion, use of $D_i(\phi,d)$ in Eq. (10) lowers the average value of the thermal exchange [15]. In the present simulations, for instance, we did not limit the maximum value of the thermal exchange energy (U_{ex}). Still, average values of 3.6, 5.1, 40.5, and 8.8 kT were obtained for U_{ex} at $\phi=0.10$, 0.20, 0.30, and 0.40, respectively, in the presence of van der Waals forces. Furthermore, at infinite dilution $D(\phi,d)\rightarrow D_0$.

In order to test the proposed model, a set of cubic three-dimensional (3D) cells composed of 125 particles was generated. Volume fractions of ($\phi=$) 0.05, 0.10, 0.15, 0.20, 0.30, 0.40, and 0.50 were produced, changing the cell length between $L=10.16a$ and $L=21.88a$ ($a=3.9\ \mu$m). Particles were randomly distributed below $\phi\leqslant 0.30$; cubic arrangements were used otherwise.

Since we are particularly interested in the decrease of the flocculation rate caused by HI's, the calculations did not include repulsive potentials. The attractive van der Waals potential (V) employed was equal to

$$V=-\frac{A}{12}\left[\frac{y}{x^2+xy+x}+\frac{y}{x^2+xy+x+y}+2\ln\left(\frac{x^2+xy+x}{x^2+xy+x+y}\right)\right], \quad (11)$$

where A is the Hamaker constant ($=1.24\times 10^{-19}$ J [68]), $x=d/2R_1$, $y=R_2/R_1$, and d is the shortest distance between the particles. The value of A was experimentally determined for Bitumen emulsions. As in previous calculations [15–19], the particles coalesce as soon as they overlap. When this happens, a new particle is created at the position of the center of mass of the colliding ones. The original volume is preserved, and the diffusion constant of the new particle at infinite dilution is recalculated in terms of the new radius according to Stokes formula [see D_0 in Eq. (3)].

For each volume fraction four types of calculations were made:

(1) Stokes: BD without HI's. This is equivalent to substitute $D(\phi,d)$ for D_0 in Eq. (10).

(2) Model: BD with the HI's of the model proposed.

(3) Batchelor: BD with HI's employing the mobility functions from Batchelor [40,41], along with Eqs. (1), (2), and (4).

(4) Honig: BD applying the correction of Honig *et al.* [Eq. (6)] between every pair of particles.

Since the random function of calculations (1), (2), and (4) do not use correlated Brownian forces, we used $R(D_0)$ for type-3 computations: that is, the random deviates comply with a Gaussian function with zero mean and variance $6D_0\Delta t$. It was shown in Ref. [15] that a reasonably large variation in the magnitude of the random forces does not change the value of the flocculation constant considerably.

''Stokes'' calculations constitute both a standard and an upper bound to the rest of the simulations, since it represents the movement of noninteracting particles at infinite dilution. ''Honig'' computations represent a lower bound since Eq. (6) is strictly applicable to binary collisions, and the cumulative use of this equation calculated by adding up contributions from every pair of particles should produce a significant underestimation of the flocculation rate. ''Model'' and ''Batchelor'' simulations are the ones we wish to compare. An additional set of simulations with $V=0$, including the different types of HI's already mentioned were also run, in order to compare the effect of the effective diffusion constant on the random deviates.

In the case of dilute systems ($\phi<0.10$), Honig-type simulations, or $V=0$ calculations, the computational time is very large. To overcome this problem, we implemented an algorithm with two time steps. A variable time step was previously suggested in Ref. [13] in order to sample a short-range (steric) potential appropriately, but allow larger displacements at long separations between the particles. In the present version, the range of the interaction potential is used as input. It was set equal to 50 nm, since beyond this distance the van der Waals attraction assumes negligible values. The value of the short time step was taken from previous simulations [15–19]. In those cases, the same van der Waals potential [Eq. (11)] was employed, along with a short-range

repulsive potential. Whenever a high repulsive barrier exists, the time step has to be varied until the number of particles is preserved in the absence of the random force [see Eq. (4)]. In the present case, t_s was taken as 1.36×10^{-6} s, although it could be chosen larger in view of the fact that the potential changes monotonically with the distance. The longer time step could be set arbitrarily high, but the accuracy of the flocculation constant will depend on that value. In the present simulations, 1.36×10^{-6} s$\leqslant t_L \leqslant 3.40\times10^{-5}$ s. Trial $\phi=0.50$ simulations at $t_s=t_L=3.40\times10^{-7}$ s were also run.

Once the long (t_L) and short (t_s) time steps are selected, a double-time-step calculation proceeds as follows: At the beginning of the simulation all particles move at t_L. The minimum separation between the particles is calculated in every iteration. If this distance is smaller than twice the preselected potential width, the particles are returned to their previous positions, and the shorter time step is used. Following, the particles move at this lower time step for t_L/t_s iterations. When this inner cycle finishes, the particles had moved for a space of t_L seconds, going back in phase with the longer time step formerly used. In this way, the coalescence of droplets can only occur in the inner cycle, where the interacting potential is properly sampled. The calculation proceeds in this way, entering the inner cycle from time to time whenever required.

FLOCCULATION RATES

A recent summary of the mechanisms of emulsion flocculation can be found in Ref. [69]. In order to estimate the flocculation constants of the computed systems, a von Smoluchowski [70] equation was used:

$$n=\frac{n_0}{1+k_f n_0 t}. \tag{12}$$

Here, n is the number of particles per unit volume, n_0 the initial particle density, t the time, and k_f a flocculation constant. In the absence of interaction forces,

$$k_f^{-1}=n_0 t_f=\frac{1}{8\pi a D_0}=\frac{3\eta}{4kT}. \tag{13}$$

At room temperature and taking water as the dispersing medium, k_f is equal to 5.49×10^{-18} m^3/s. This value increases in the presence of van der Waals forces and decreases as a consequence of repulsive forces and/or HI's. The variation of clusters of different sizes as a function of time closely follows the predictions of von Smoluchowski [70], although there is still some discrepancy about the exact values of the flocculation rate constants k_{ij} between flocs of i and j particles, respectively [54,71–73]. The most precise validations of the theory come from single [71] and multiparticle [72,73] light scattering measurements.

Equation (12) strictly applies to the process of flocculation only. It does not consider the process of coalescence that may occur at a different rate. We studied in the past other formalisms [74,75] to account for coalescence as well as flocculation [18,19]. The generalization of the former treatment [70] including both processes was already published by Danov *et al.* [76]. The definition of coalescence implies the existence of a finite time for the drainage of the intervening liquid between colliding drops. However, in our simulations both flocculation and coalescence are included in the effective value of k_f. In the present case where coalescence occurs instantaneously after the droplets overlap there is no ambiguity over the nature of the flocculation constant. In more involved cases where there exists a repulsive barrier or a finite drainage time, comparison between the values of k_f calculated with and without such a barrier and flux will evidence the effect of coalescence on the flocculation rate. Since drops increase their size by coalescence as they collide in a similar way as solid particles form bigger flocs with larger hydrodynamic radii, aggregates weigh the same as larger particles in Eq. (12), and k_f can be evaluated using an algorithm that incorporates instantaneous coalescence [15].

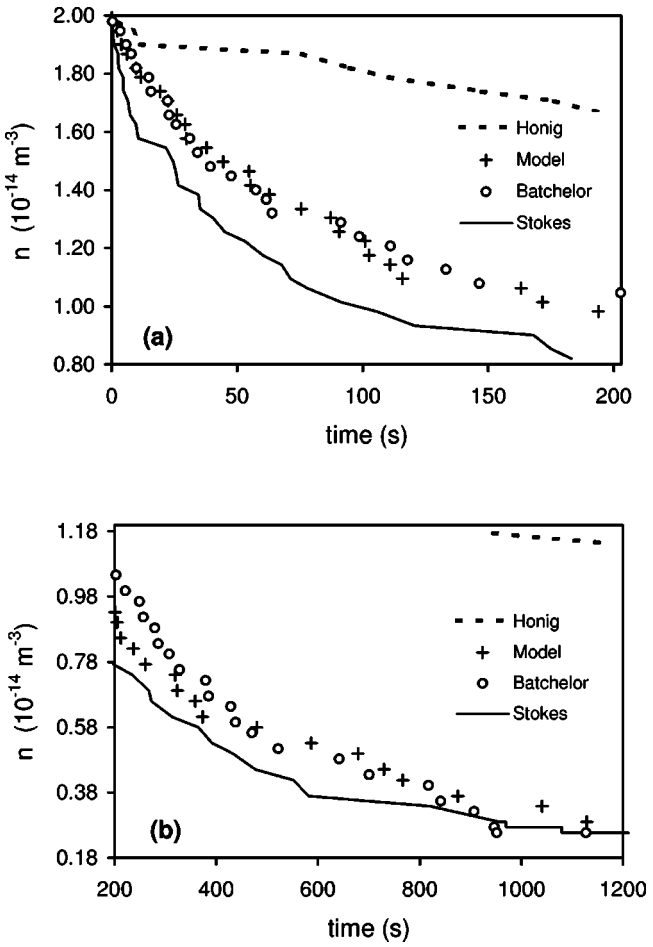

FIG. 3. Number of particles per unit volume (n), as a function of time (t) for $\phi=0.05$. (a) $t\leqslant200$ s, (b) $t\geqslant200$ s.

RESULTS

Figure 3 shows the variation of the number of particles per unit volume (n) as a function of time for $\phi=0.05$. At low volume fractions the tensor (Batchelor) and model prediction (Model) approach Stokes' result. As expected, the cumulative use of the formula of Honig *et al.* slows down floccula-

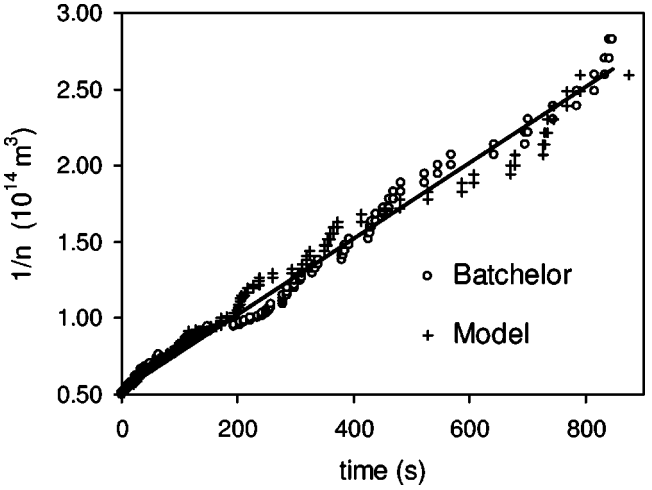

FIG. 4. $1/n$ vs t for $\phi=0.05$ [Eq. (12)].

tion considerably and sets an upper bound to the variation of n vs t.

According to Eq. (12), plot of $1/n$ vs t should produce a straight line with a slope equal to k_f (see Fig. 4). Following this procedure, values of $k_f=2.49\times10^{-17}$ m^3/s ($r^2=0.9900$) and $k_f=2.36\times10^{-17}$ m^3/s ($r^2=0.9894$) were obtained for Batchelor and Model calculations, respectively. As viewed in Fig. 3 the dispersion of the data increases as the number of particles diminishes. In general, high volume fractions and high flocculation rates decrease the quality of the fitting [Eq. (12)] due to multiple collisions [15–19]. In any case, only part of the data can be used for the computation of the flocculation constant. When the number of particles (N) decreases considerably ($N<20$), the flocculation behavior does not obey the predictions of Eq. (12). A larger number of particles can diminish this effect by extending the range of usable data. Unfortunately they can also be very time consuming. Figure 5 shows a plot of $1/n$ vs t for 1000 particles at $\phi=0.30$. This calculation took more than 2 months in a

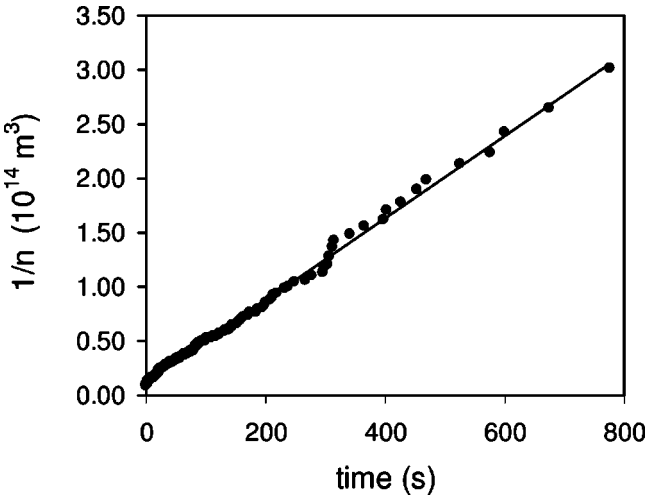

FIG. 5. $1/n$ vs t for $\phi=0.15$. In this calculation 1000 particles were used. Neither HI's nor van der Waals forces were included. Only random forces were taken into account.

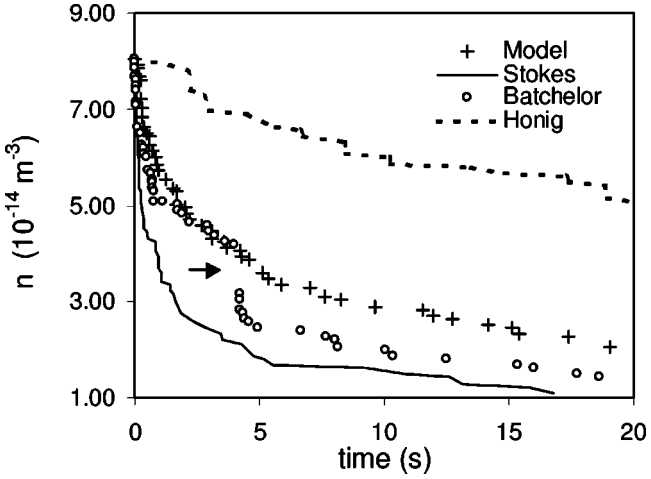

FIG. 6. n vs t for $\phi=0.20$. The tensor prediction (Batchelor) undergoes a drastic variation in the number of particles after $n=4.12\times10^{14}$ m^{-3} (arrow) as a consequence of a multiple collision induced by the overestimation of HI's at short distances.

Dell 5300, employing a single time step, and only a random force without HI's. For this case $k_f=3.77\times10^{-17}$ m^3/s ($r^2=0.9961$). This regression coefficient is considerably better to that of similar calculations with a smaller number of particle [15]. As shown in Ref. [15], the value of k_f depends markedly on the volume fraction, approaching the limit of 5.49×10^{-18} m^3/s as $\phi\rightarrow0$, in the absence of a repulsive barrier.

As the volume fraction increases, the chance of a multiple collisions also increases. Figure 6 shows a plot of n vs t for $\phi=0.20$. The present methodology for HI's varies monotonically, sensibly separated from the Stokes prediction. The Batchelor prediction coincides with the Model prediction until $t=4.22$ s ($n=4.12\times10^{14}$: see Fig. 6). At that time, overestimation of the diffusion matrix elements causes a multiple-particle collision that decreases the density of particles appreciably. Shortly after the drastic drop of n, the tensorial prediction recovers the slope of the Model approach.

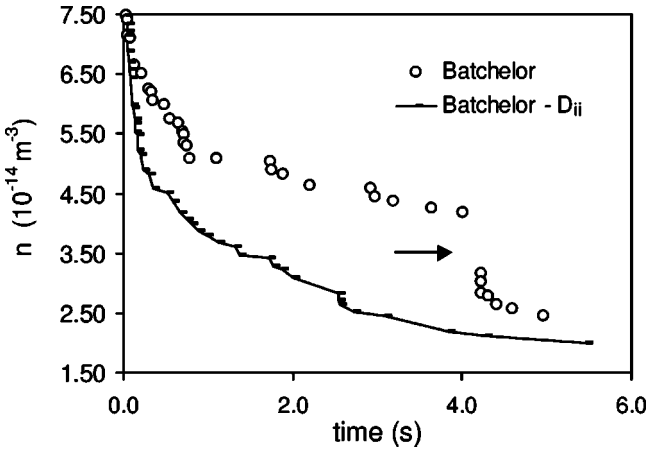

FIG. 7. Tensorial prediction of n vs t for $\phi=0.20$, calculated with (○) the whole diffusion matrix and (−) the diagonal elements (D_{ii}) of the diffusion matrix.

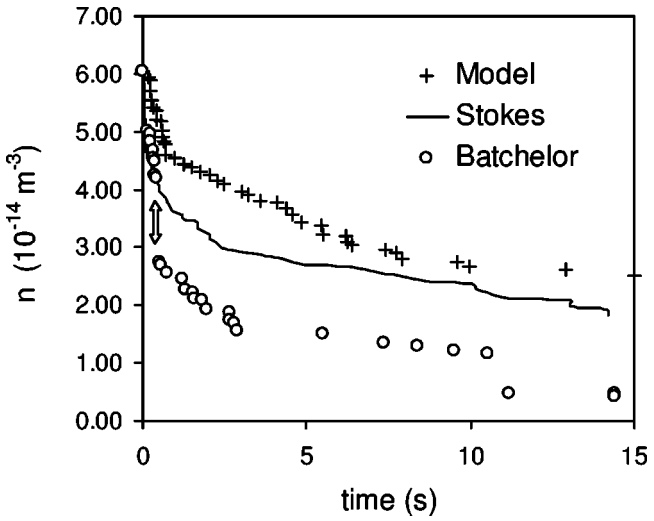

FIG. 8. n as a function of time for $\phi=0.15$. The overestimation of HI's produces an abrupt change in the number of particles that carries the tensorial prediction below the Stokes estimation.

In order to avoid the referred to anomaly we did several tests in which (a) only the diagonal elements of the diffusion matrix are used, (b) only nondiagonal elements are used, (c) the values of the diagonal or nondiagonal elements were multiplied by a number lower than 1.0, and (d) a critical cutoff radius for the HI's was defined. In this latter case (d), D_0 was employed at distances lower than R_{critical}, and Batchelor tensor was employed otherwise. It appears that the major overestimation of HI's comes from the nondiagonal elements. Figure 7 shows the complete Batchelor prediction for $\phi=0.20$ (from Fig. 6), along with the ''diagonal'' correction. The anomalous variation in n is avoided, but the flocculation rate is overestimated. Furthermore, even the most successful corrections [(a) and (d)] failed at longer times and/or different systems. Figure 8 ($\phi=0.15$) shows that this phenomenon can also occur in more dilute systems and is rather configuration dependent. In this case, the drop in the number of particles is so severe that the tensorial prediction comes out to be faster than the Stokes result.

Table I shows the values of the flocculation constant, calculated from fitting of $1/n$ vs t plots (whenever possible). The values of k_f for $\phi\leqslant 0.30$ corresponding to the proposed model, Stokes and Honig *et al.* [47], increase steadily with ϕ, while that of the tensor does not. Furthermore, the predictions of the model always fall between the limits of Stokes

TABLE I. Flocculation constants calculated from linear fits of $1/n$ vs t plots.

ϕ $\times 100$	k_f (m^3/s) Stokes	k_f (m^3/s) Batchelor	k_f (m^3/s) Model	k_f (m^3/s) Honig
5	3.33×10^{-17}	2.49×10^{-17}	2.36×10^{-17}	3.13×10^{-18}
10	8.24×10^{-17}	4.15×10^{-17}	5.49×10^{-17}	2.87×10^{-18}
15	1.65×10^{-16}	1.45×10^{-15}	1.37×10^{-16}	9.59×10^{-18}
20	8.12×10^{-16}	4.47×10^{-16}	1.64×10^{-16}	9.47×10^{-18}
30	1.29×10^{-14}	2.22×10^{-15}	8.09×10^{-16}	2.59×10^{-15}

TABLE II. Flocculation rates deduced from the values of $t_{1/2}$ through Eq. (14).

ϕ $\times 100$	k_f (m^3/s) Stokes	k_f (m^3/s) Batchelor	k_f (m^3/s) Model	k_f (m^3/s) Honig
5	5.43×10^{-17}	2.25×10^{-17}	2.90×10^{-17}	3.06×10^{-18}
10	1.31×10^{-16}	7.31×10^{-17}	6.46×10^{-17}	2.98×10^{-18}
15	6.89×10^{-16}	4.18×10^{-15}	2.59×10^{-16}	1.39×10^{-17}
20	1.48×10^{-15}	2.94×10^{-16}	2.94×10^{-16}	1.44×10^{-17}
30	1.09×10^{-14}	2.82×10^{-15}	1.89×10^{-15}	1.36×10^{-16}
40	4.89×10^{-15}	1.79×10^{-15}	7.36×10^{-16}	2.26×10^{-17}
50	7.22×10^{-13}	2.11×10^{-13}	2.70×10^{-14}	2.59×10^{-15}

and Eq. (5). It should be stressed again that the equations of Honig *et al.* are only valid for binary collisions. The calculation of coefficient β [in Eq. (5)] as a sum of binary contributions from all surrounding particles is an approximation that largely overestimates the effect of HI's. Hence, the values identified as ''Honig'' in Tables I and II show differences of more than one order of magnitude with all the rest.

For volume fractions larger than 0.30, the shape of the n vs t curves changes significantly. Since each particle is closely surrounded by its neighbors (the maximum volume fraction is equal to $\phi=0.52$ for cubic packing of monodispersed spheres), its movement is severely affected by HI's. This generates a lag time: a finite time between the beginning of the simulation and the start of a sharp decrease in n (see Fig. 9). When the number of particles changes, it decreases in the form of a step function and does not present the characteristic convexity predicted by Eq. (12). This drastic reduction of the flocculation rate at large volume fractions is consistent with the decrease in the creaming velocity of similar emulsions ($a_i=0.86\ \mu$m) for $\phi\geqslant 0.40$ [77]. It could also be related to the variation of the average droplet size in

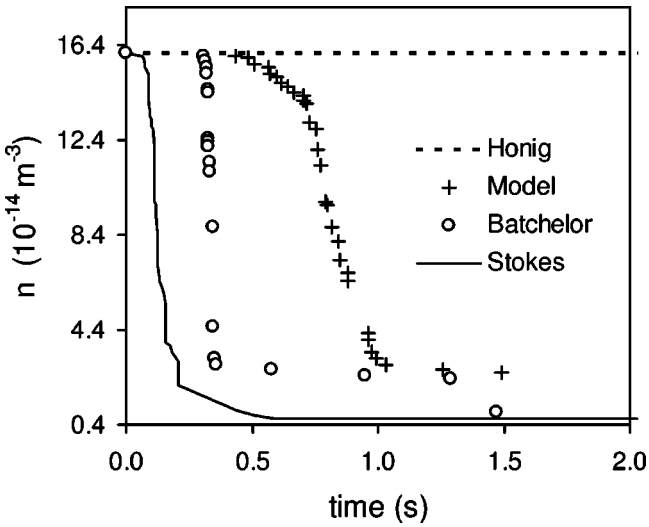

FIG. 9. At $\phi\geqslant 0.40$, the curves of n vs t change their shape. A lag time is generated as a consequence of a severe slow down in particle movement at the beginning of the simulation. The variation of n vs t is abrupt. The typical concave shape predicted by Eq. (12) is not observed.

hydrocarbon oil-water emulsions stabilized with β-lactoglobulin [8]. As shown in the Fig. 4a of Ref. [8], the average drop size of the emulsion may remain stable under shearing for a period of 3 h after preparation, increasing drastically afterwards from 0.36 μm to 4.5 μm in the following 20 min.

It can be observed in Fig. 9 that in contrast to the results from Fig. 8, Batchelor predictions are slower than Stokes ones. This evidences that the particular behavior of the tensor previously referred to depends on the configuration on the surrounding particles and not necessarily on the total volume fraction of the system. It is important to point out that the overestimation of HI's is not due to the specific form of the mobility functions from Batchelor, since Rotne-Prager's and Oseen's were also tested.

In order to estimate the flocculation constant for high-volume-fraction calculations, a simple relationship between this variable and the time necessary to diminish the number of drops to half its original value was used:

$$k_f = \frac{1}{n_0 t_{1/2}}, \tag{14}$$

where $t_{1/2} = t(n_0/2)$, the time required for the number of particles, n, to drop to $\frac{1}{2}\, n_0$. Equation (14) easily follows from Eq. (12) substituting n by $n_0/2$. The values of k_f obtained in this way are not very accurate due to fast decay in the number of particles with time. When multiple collisions occur, the time for which $n = n_0/2$ cannot always be determined. Since the number of particles is directly read from the simulations, we used the closest approximation to $n_0/2$ whenever this value was not available. The trends from Tables I and II are similar, except that the value of k_f predicted by the model for $\phi = 0.40$ is lower than that of $\phi = 0.30$ for the reasons just explained.

CONCLUSIONS

A simple methodology for the calculation of HI's in Brownian dynamics simulations of concentrated systems was proposed. The model overcomes the shortcomings of the tensorial calculations previously outlined by Heyes [20]. Specifically, it clearly avoids overestimation of the HI's by superposition of pair contributions. The calculated values of the flocculation rates appear to be reasonable (the order of magnitude is appropriate), although direct comparison with experimental data from Bitumen emulsions ($A = 1.24 \times 10^{-19}$ J, $a = 3.9$ μm [68]) was not possible.

Modifications of the present technique for the treatment of deformable droplets and particle-wall interactions are possible. In a first approximation, the latter case could be treated using the present methodology. For this case, the volume fraction of the wall inside the region $R_{\text{int}} < d' \leqslant R_{\text{ext}}$ could be included in the local volume fraction calculation around the particle. At shorter separations $d' < R_{\text{int}}$, similar relations as those of Eqs. (5) and (6) are expected to hold, since they were originally deduced for a particle-surface interaction [45]. However, the coefficients of a rational function for the HI's between a particle and a surface can be very different. This is illustrated in Table 1 of Ref. [48], in which case, a third-order rational function was used to substitute the infinite series result given by Brenner [45,46] for the sphere-sphere and sphere-plane surface systems.

[1] D. Ermak and J.A. McCammon, J. Chem. Phys. **69**, 1352 (1978).

[2] J. Bacon, E. Dickinson, and R. Parker, J. Chem. Soc., Faraday Trans. 2 **79**, 91 (1983).

[3] E. Dickinson, J. Chem. Soc., Faraday Trans. 2 **75**, 466 (1979).

[4] H.C. Öttinger, Phys. Rev. E **50**, 2696 (1994).

[5] M. Whittle and E. Dickinson, Mol. Phys. **90**, 739 (1997).

[6] E. Dickinson, in *The Structure, Dynamics and Equilibrium Properties of Colloidal Systems*, edited by D.M. Bloor and E. Wyn-Jones (Kluwer Academic, Dordrecht, 1990), pp. 707–727.

[7] H. Oshima, T.W. Healy, and L.R. White, J. Chem. Soc., Faraday Trans. 2 **80**, 1299 (1984).

[8] J. Chen, E. Dickinson, and G. Iveson, Food Struct. **12**, 135 (1993).

[9] M.R. Oberholzer, N.J. Wagner, and A.M. Lenhoff, J. Chem. Phys. **107**, 9157 (1997).

[10] W. Nuesser and H. Versmold, Mol. Phys. **96**, 893 (1999).

[11] A.M. Puertas, J.A. Maroto, A. Fernández-Barbero, and F.J. de las Nieves, Colloids Surf., A **151**, 473 (1999).

[12] M. Hütter, Phys. Chem. Chem. Phys. **1**, 4429 (1999).

[13] M. Romero-Cano, A.M. Puertas, and F.J. de las Nieves, J. Chem. Phys. **112**, 8654 (2000).

[14] A.M. Puertas, A. Fernández-Barbero, and F.J. de las Nieves, Comput. Phys. Commun. **121**, 353 (1999).

[15] G. Urbina-Villalba, M. García-Sucre, and J. Toro Mendoza, Mol. Simul. **29**, 393 (2003).

[16] G. Urbina-Villalba and M. García-Sucre, Langmuir **16**, 7975 (2000).

[17] G. Urbina-Villalba and M. García-Sucre, Colloids Surf., A **190**, 111 (2001).

[18] G. Urbina-Villalba and M. García-Sucre, Interciencia **25**, 415 (2000).

[19] G. Urbina-Villalba and M. García-Sucre, Mol. Simul. **27**, 75 (2001).

[20] D.M. Heyes, Mol. Phys. **87**, 287 (1996).

[21] M.P. Allen and D.J. Tildesley, *Computer Simulation of Liquids* (Oxford University Press, New York, 1987).

[22] W.B. Russel, D.A. Saville, and W.R. Schowalter, *Colloidal Dispersions* (Cambridge University Press, Cambridge, England, 1989).

[23] P.J. Hoogerbrugge and J.M.V.A. Koelman, Europhys. Lett. **19**, 155 (1992).

[24] P. Español, Phys. Rev. E **52**, 1734 (1995).

[25] A. Einstein, in *Investigations on the Theory of Brownian Movement*, edited by R. Fürph (Dover, New York, 1956); Ann.

Phys. (Leipzig) **17**, 549 (1957).
[26] S. Chandrasekhar, Rev. Mod. Phys. **15**, 1 (1943).
[27] M.C. Wang and G.E. Uhlenbeck, Rev. Mod. Phys. **17**, 323 (1945).
[28] R. Kubo, J. Phys. Soc. Jpn. **12**, 570 (1957).
[29] I.B. Ivanov, K.D. Danov, and P.A. Kralchevsky, Colloids Surf., A **152**, 161 (1999).
[30] A. Kabalnov, J. Dispersion Sci. Technol. **22**, 1 (2001).
[31] T.M. Squires and M.P. Brenner, Phys. Rev. Lett. **85**, 4976 (2000).
[32] E.R. Dufresne, T.M. Squires, M.P. Brenner, and D.G. Grier, Phys. Rev. Lett. **85**, 3317 (2000).
[33] J.R. Melrose and R.C. Ball, Europhys. Lett. **32**, 535 (1995).
[34] H. Tanaka and T. Araki, Phys. Rev. Lett. **85**, 1338 (2000).
[35] G. Nägele and P. Baur, Europhys. Lett. **38**, 557 (1997).
[36] B. Rinn, K. Zhan, P. Maass, and G. Maret, Europhys. Lett. **46**, 537 (1999).
[37] J.K.G. Dhont, *An Introduction to Dynamics of Colloids* (Elsevier Science B.V., Amsterdam, 1996), Chaps. 3 and 5.
[38] T.G.M. van de Ven, *Colloidal Hydrodynamics* (Academic, Padstow, 1989), Chaps. 1 and 2.
[39] J. Rotne and S. Prager, J. Chem. Phys. **50**, 4831 (1969).
[40] G.K. Batchelor, J. Fluid Mech. **119**, 379 (1982).
[41] G.K. Batchelor, J. Fluid Mech. **74**, 1 (1976).
[42] D.M. Heyes and A.C. Branka, Mol. Phys. **98**, 1949 (2000).
[43] R.M. Jendrejack, M.D. Graham, and J.J. de Pablo, J. Chem. Phys. **113**, 2894 (2000).
[44] W.H. Press, S.A. Teukolsky, W.T. Vetterling, and B.P. Flannery, *Numerical Recipes in Fortran 77* (Cambridge University Press, New York, 1999), Vol. 1, Chap. 7, pp. 279–287.
[45] H. Brenner, Chem. Eng. Sci. **16**, 242 (1961).
[46] A.J. Goldman, R.G. Cox, and H. Brenner, Chem. Eng. Sci. **21**, 1151 (1966).
[47] E.P. Honig, G.J. Roebersen, and P.H. Wiersema, J. Colloid Interface Sci. **36**, 97 (1971).
[48] D.Y.C. Chan and B. Halle, J. Colloid Interface Sci. **102**, 400 (1984).
[49] K. Zahn, J.M. Méndez-Alcaraz, and G. Maret, Phys. Rev. Lett. **79**, 175 (1997).
[50] J. Meiners and S.R. Quake, Phys. Rev. Lett. **82**, 2211 (1999).
[51] M. Kollmann and G. Nägele, Europhys. Lett. **52**, 474 (2000).
[52] J.C. Crocker, J. Chem. Phys. **106**, 2837 (1997).
[53] P. Bartlett, S.I. Henderson, and S.J. Mitchell, Philos. Trans. R. Soc. London, Ser. A **359**, 883 (2001).
[54] H. Holthoff, S.U. Egelhaaf, M. Borkovec, P. Schurtenberger, and H. Sticher, Langmuir **12**, 5541 (1996).
[55] A.M. Puertas and F.J. de las Nieves, J. Colloid Interface Sci. **216**, 221 (1999).
[56] J. Bacon, E. Dickinson, and R. Parker, Faraday Discuss. Chem. Soc. **76**, 165 (1983).
[57] A.B. Glendinning and W.B. Russel, J. Colloid Interface Sci. **89**, 124 (1982).
[58] D.O. Riese, G.H. Wegdam, W.L. Vos, R. Sprik, D. Feinstein, J.H.H. Bonguerts, G. Grubel, Phys. Rev. Lett. **85**, 5460 (2000).
[59] H. Auweter and D. Horn, J. Colloid Interface Sci. **105**, 399 (1985).
[60] A. van Veluwen, H.N.W. Lekkerkerker, C.G. de Kruif, and A. Vrij, Faraday Discuss. Chem. Soc. **83**, 59 (1987).
[61] W. van Megen, S.M. Underwood, R.H. Ottewill, N.St.J. Williams, and P.N. Pusey, Faraday Discuss. Chem. Soc. **83**, 47 (1987).
[62] P.N. Pusey and W. van Megen, J. Phys. (Paris) **44**, 285 (1983).
[63] B.U. Felderhof, Physica A **89**, 373 (1977).
[64] B.U. Felderhof, J. Phys. A **11**, 929 (1978).
[65] C.W.J. Beenakker and P. Mazur, Phys. Lett. A **91**, 290 (1982).
[66] C.W.J. Beenakker and P. Mazur, Physica A **126**, 349 (1984).
[67] P. Español and P. Warren, Europhys. Lett. **37**, 511 (1997).
[68] M. Salou, B. Siffert, and A. Jada, Colloids Surf., A **142**, 9 (1998).
[69] D.N. Petsev, in *Encyclopedia of Surface and Colloid Science* (Dekker, New York, 2002), pp. 3192–3207.
[70] M. von Smoluchowski, Z. Phys. Chem. **92**, 129 (1917).
[71] H. Sonntag, and K. Strenge, *Coagulation Kinetics and Structure Formation* (VEB Deutscher Verlag der Wissenschaften, Berlin, 1987).
[72] H. Sonntag, V. Shilov, H. Gedan, H. Lichtenfeld, and C. Dürr, Colloids Surf. **20**, 303 (1986).
[73] H. Holthoff, A. Schmitt, A. Fernández-Barbero, M. Borkovec, M.A. Cabrerízo-Vílchez, P. Schurtenberger, and R. Hidalgo-Alvarez, J. Colloid Interface Sci. **192**, 463 (1997).
[74] M. van den Tempel, Recueil **72**, 433 (1953).
[75] R.P. Borwankar, L.A. Lobo, and D.T. Wasan, Colloids Surf. **69**, 135 (1992).
[76] K.D. Danov, I.B. Ivanov, T.D. Gurkov, and R. Borwankar, J. Colloid Interface Sci. **167**, 8 (1994).
[77] R. Chanamai and D.J. McClements, Colloids Surf., A **172**, 79 (2000).